CHEMISTRY
A EUROPEAN JOURNAL

DOI: 10.1002/chem.200701068

Azulene-Moiety-Based Ligand for the Efficient Sensitization of Four Near-Infrared Luminescent Lanthanide Cations: Nd^{3+}, Er^{3+}, Tm^{3+}, and Yb^{3+}

Jian Zhang and Stéphane Petoud*[a]

Abstract: The ML_4 complexes formed by reaction between the bidentate azulene-based ligand diethyl 2-hydroxyazulene-1,3-dicarboxylate (HAz) and several lanthanide cations (Pr^{3+}, Nd^{3+}, Gd^{3+}, Ho^{3+}, Er^{3+}, Tm^{3+}, Yb^{3+}, and Lu^{3+}) have been synthesized and characterized by elemental analysis, FT-IR vibrational spectroscopy and electrospray ionization mass spectroscopy. Spectrophotometric titrations have revealed that four Az^- ligands react with one lanthanide cation to form the ML_4 complex in solution. Studies of the luminescence properties of these ML_4 complexes demonstrated that Az^- is an efficient sensitizer for four different near-infrared emitting lanthanide cations (Nd^{3+}, Er^{3+}, Tm^{3+}, and Yb^{3+}); the resulting complexes have high quantum yield values in CH_3CN. The near-infrared emission arising from Tm^{3+} is especially interesting for biologic imaging and bioanalytical applications since biological systems have minimal interaction with photons at this wavelength. Hydration numbers, representing the number of water molecules bound to the lanthanide cations, were obtained through luminescence lifetime measurements and indicated that no molecules of water/solvent are bound to the lanthanide cation in the ML_4 complex in solution. The four coordinated ligands protect well the central luminescent lanthanide cation against non-radiative deactivation from solvent molecules.

Keywords: azulenes · lanthanides · luminescence · near-infrared spectroscopy · sensitizers

Introduction

The development of near-infrared (NIR) emitting lanthanide complexes in both aqueous and non-aqueous media (with $Ln^{3+} = Nd^{3+}$, Yb^{3+}, Er^{3+}, Ho^{3+}, Tm^{3+}, and Pr^{3+}) is an increasingly active research area in recent years.[1–23] As an example, NIR emission is advantageous for biological applications because i) NIR photons scatter less than visible photons for improved biological imaging resolution),[24] ii) biological systems have low native autofluorescence in the NIR domain for better signal-to-noise ratio and corresponding detection sensitivity,[25] and iii) biological tissues are almost transparent to NIR light (NIR photons travel deep (several centimeters) in tissues, organs or organisms).[25,26] NIR lanthanide luminescence can also be advantageously used in NIR organic light-emitting diode technology[27,28] and telecommunication where the electronic structure of lanthanide ions such as Er^{3+}, Nd^{3+} and Ho^{3+} can be used as the active material for optical amplifiers of NIR signals.[29,30]

The luminescence signals of lanthanide ions originate from their f–f electronic transitions within the partially filled 4f orbitals. The electronic levels of lanthanides are hardly affected by their surrounding environment because of the shielding effect of the 4f electrons by the filled 5s and 5p orbitals.[1,2] These transitions are spin-forbidden, resulting in emissions that appear as sharp line-like bands, a useful advantage for spectral discrimination between signals of the sample from the background fluorescence for improved signal-to-noise ratio and detection sensitivity. Free lanthanide cations have low absorption coefficients and long intrinsic luminescence lifetimes ("radiative lifetimes" from microseconds to milliseconds).[1,2] In order to generate sufficient emission signal for sensitive detection, lanthanide cations need to be sensitized with a suitable antenna that possesses the appropriate electronic structure[31] and efficiently protected from high energy vibrations to prevent the non-radiative deactivation of the lanthanide luminescence. The sensitization process of luminescent lanthanide cations in coordination complexes formed with chromophoric ligands can usually be described as resulting from the excitation of

[a] J. Zhang, Prof. Dr. S. Petoud
Department of Chemistry, University of Pittsburgh
219 Parkman Ave., Pittsburgh, PA 15260 (USA)
Fax: (+1) 412-624-8611
E-mail: spetoud@pitt.edu

Supporting information for this article is available on the WWW under http://www.chemeurj.org/ or from the author.

the sensitizer (antenna) by absorption of photons through the singlet states of the chromophoric group, followed by the internal ligand-centered energy conversion via intersystem crossing from the singlet to the triplet state. The energy is then transferred from the triplet state of the ligand to the accepting levels of the lanthanide ions. Energy transfer from the singlet state to the lanthanide is also possible.[17,32,33] Because the accepting energy levels of NIR emitting lanthanide ions are generally located at lower energy compared with visible emitting lanthanides, we hypothesized that efficient sensitizing ligands for NIR emitting lanthanide cations should have a triplet state located at relatively lower energy. As reference, we have previously studied the tropolonate (Trop-) ligand which possesses a triplet state located at an energy of 17200 cm^{-1} (580 nm) for the sensitization of several NIR emitting lanthanide ions.[34]

Azulene is a non-benzenoid aromatic molecule; its name is derived from the Spanish word "azul", meaning blue. It is a dark blue crystalline solid used in many cosmetics. Azulene is an isomer of naphthalene but its photophysical properties are significantly different. Its structure consists of a cyclopentadiene ring fused with a cycloheptatriene ring, and can be therefore considered as a fusion product of a 4π electrons cyclopentadienide anion which is aromatic and the corresponding aromatic 6π electrons tropylium cation (Scheme 1). Due to this particular electronic structure, azulene appears to be a versatile organic fragment with both an electron-rich five-membered ring that could act as a potential electron density donor and an electron-deficient seven-membered ring that could act as a potential electron density acceptor. Due to this rich electronic character, azulene and its derivatives have been attracting a growing interest in various areas of molecular materials, such as charge transfer complexes,[35,36] conducting polymers,[37,38] liquid crystals,[39,40] anion receptor/sensors,[41,42] optoelectronic molecular switches,[43] as well as nonlinear optical (NLO) material.[44–46]

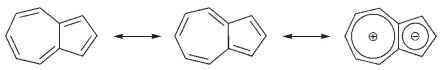

Scheme 1. Azulene and its polar resonance molecular structure.

For the sensitization of NIR emitting lanthanide cations, the azulene moiety is interesting since it possesses a triplet state located at significantly lower energy (13600 cm^{-1}),[47] in comparison to the tropolonate ligand (17200 cm^{-1}). It is therefore hypothesized that azulene would have better sensitizing efficiency for NIR lanthanides since its triplet state is located at lower energy, closer to the energy of accepting levels of several NIR emitting lanthanide cations. In this work, we have designed and synthesized a new bidentate ligand that incorporates the azulene moiety (Scheme 2): diethyl 2-hydroxyazulene-1,3-dicarboxylate (HAz; synthesized according to Scheme 3), for the coordination and sensitization of NIR emitting lanthanide cations. The synthesis of the ligand and several of its lanthanide complexes are reported in this paper. The luminescent properties have been analyzed and quantified. The ligand Az^- has been demonstrated to act as an efficient sensitizer for several different lanthanide ions emitting in the near-infrared: Yb^{3+}, Nd^{3+}, Er^{3+}, as well as Tm^{3+}. It is worth noting that Tm^{3+} luminescence arising from a complex in solution is rarely reported, and luminescence is especially appealing for bioimaging, since its main NIR emission band is located around 800 nm, which corresponds to an absorption minimum for water and tissues.[25,26]

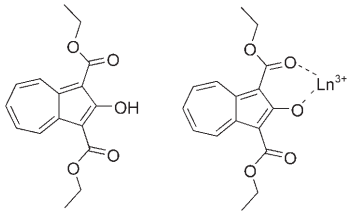

Scheme 2. Structure of the ligand HAz and proposed bidentate coordination mode of Az^- with lanthanide ion.

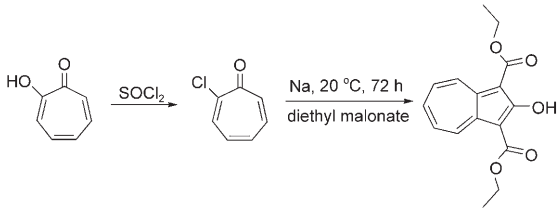

Scheme 3. Synthesis of ligand HAz.

Experimental Section

Materials: All reagents were used as received, unless otherwise stated. Tropolone, thionyl chloride, diethyl malonate, $LnCl_3{\cdot}nH_2O$ (Ln = Nd, Gd, Er, Tm, and Yb, 99.9% or 99.99%, $n = 6$ or 7 depending on the Ln), and KOH standardized solution in methanol (0.100 N) were purchased from Aldrich. All deuterated NMR solvents were purchased from Cambridge Isotope Labs and used as received. $KGd(Trop)_4$ was prepared according to our published procedure.[34]

Methods: Infrared spectra were recorded on a Perkin-Elmer Spectrum BX FT-IR instrument. Samples were prepared with a drop of dichloromethane solution, and evaporated to dryness on KBr pellets. Elemental analyses were performed by Atlantic Microlab, Inc. (Norcross, Georgia). ^1H NMR spectra were recorded on a Bruker DPX-300 spectrometer at 300 MHz. MS-EI and MS-ESI were measured on a Micromass Autospec and Agilent HP 1100 series LC-MSD instruments respectively. UV/Vis absorption spectra were recorded on a Perkin-Elmer Lambda 19 spectrophotometer.

Spectrophotometric titration: Spectrophotometric titrations were performed with a Perkin–Elmer Lambda 19 spectrophotometer connected to an external computer. All titrations were performed in a 1.00 cm thermostated (25.0 ± 0.1 °C) cuvette in CH_3OH or CH_3CN at constant ionic strength $\mu = 0.01$ M (tetrabutylammonium perchlorate). In a typical experiment, 2.00 mL of a ligand solution in CH_3OH (initial total ligand concentration 1×10^{-5} M) was titrated with $LnCl_3$ solutions, (stock solution concentration: 2×10^{-5} M in CH_3OH). The kinetic of formation of the complexes was tested to take place within one minute by monitoring the changes through UV/Vis absorption spectra. For the titration experiments, two minutes after each addition of aliquot of the lanthanide salt stock solution to the ligand solution, the UV/Vis spectrum of the result-

ing solution was recorded. Factor analysis and mathematical treatment of the spectrophotometric data were performed with the SPECFIT program.[48]

Luminescence measurements: Emission and excitation spectra were measured using a JY Horiba Fluorolog-322 spectrofluorometer equipped with a Hamamatsu R928 detector for the visible domain and an Electro-Optical Systems, Inc. DSS-IGA020 L detector for the NIR domain. The NIR luminescence relative quantum yields were measured by using KYb(Trop)$_4$ complex ($\Phi = 1.9 \times 10^{-2}$ in DMSO) as reference.[34] Spectra were corrected for the instrumental function for both excitation and emission. Values were calculated using the following equation:

$$\frac{\Phi_x}{\Phi_r} = \frac{A_{r(\lambda r)}}{A_{x(\lambda x)}} \frac{I_{(\lambda r)}}{I_{(\lambda x)}} \frac{\eta_x^2}{\eta_r^2} \frac{D_x}{D_r}$$

where subscript r stands for the reference and x for the sample; A is the absorbance at the excitation wavelength, I is the intensity of the excitation light at the same wavelength, η is the refractive index ($\eta = 1.478$ in DMSO, $\eta = 1.344$ in acetonitrile, $\eta = 1.342$ in CD_3CN), and D is the measured integrated luminescence intensity. The luminescence lifetime measurements were performed by excitation of solutions in 1 cm quartz cells using a Nd/YAG Continuum Powerlite 8010 Laser at 354 nm (third harmonic) as excitation source. Emission was collected at a right angle to the excitation beam, the emission wavelength selected with a Spectral Products CM 110 1/8 meter monochromator. The signal was monitored by a cooled photomultiplier (Hamamatsu R316–2) coupled to a 500 MHz bandpass digital oscilloscope (Tektronix TDS 754D). The signals to be treated (at least 15000 points resolution for each trace) were averaged from at least 500 individual decay curves. Luminescence decay curves were imported into Origin 7.0 scientific data analysis software. The decay curves were analyzed using the Advanced Fitting Tool module. Reported luminescence lifetimes are averages of at least three independent determinations.

2-Chlorocyclohepta-2,4,6-trien-1-one: The title compound was synthesized according to the method described by Brettle et al.[49] and Doering et al.[50] Tropolone (1.00 g, 8.20 mmol) was dissolved in dry benzene (25 mL) to give a colorless solution. Thionyl chloride (1.07 g, 8.99 mmol) was then added, which immediately give a white precipitate of tropolone hydrogen chloride; the precipitate dissolved after heating under reflux for 1.5 h to afford a dark-red solution. Excess thionyl chloride and benzene were evaporated and the brown residue was washed with hexane and evaporated. After chromatography (silica gel, 35% hexanes/ethyl acetate), 2-chlorotropone was obtained as a white solid (1.07 g, 94%). M.p. 64–65 °C; ^{1}H NMR (CD_3COCD_3, 300 MHz): $\delta = 7.93$ (d, $J = 9.3$ Hz, 1H), 7.41–7.34 (m, 1H), 7.25–7.04 ppm (m, 3H); IR (KBr): $\tilde{\nu} = 3568$ ($\nu_{O\text{-}H}$), 3215 ($\nu_{C\text{-}H}$), 1603 ($\nu_{C=O}$), 1591 ($\nu_{C=O}$), 1544, 1477, 1458, 1413, 1361, 1306, 1242, 1204, 1076, 994, 957, 897, 778, 749 cm^{-1}; EI-MS: m/z: calcd for 140.002893; found: 140.003216 $[M]^+$.

Diethyl 2-hydroxyazulene-1,3-dicarboxylate: The title compound was synthesized according to the method described by Brettle et al.[49] To a sodium ethoxide solution prepared from sodium (700 mg) and absolute ethanol (50 mL), diethyl malonate (2.4 g) and 2-chlorotropone (700 mg) were added, and the mixture was allowed to stand for 72 h at room temperature. The reaction mixture turned into a gelatinous orange mass. Water was then added to this suspension, and the sodium salt of the targeted compound precipitated out. After collection by filtration, the precipitate was redissolved in glacial acetic acid. This solution was diluted with water and extracted with chloroform. The solvent was then evaporated and the residue was recrystallized from ethanol to give orange-yellow needles (720 mg, 50%). M.p. 95 °C; ^{1}H NMR (CD_3COCD_3, 300 MHz): $\delta = 1.45$ (t, $J = 7.2$ Hz, 6H), 4.48 (q, $J = 7.2$ Hz, 4H), 7.84–7.93 (m, 3H), 9.44–9.47 (m, 2H), 11.68 ppm (s, 1H); IR (KBr): $\tilde{\nu} = 2978$, 1671 ($\nu_{C=O}$), 1650 ($\nu_{C=O}$), 1597, 1533, 1476, 1435, 1333, 1284, 1204, 1176, 1032, 799, 735 cm^{-1}; EI-MS: m/z: calcd for 288.099774; found: 288.100211 $[M]^+$.

Lanthanide complexes: To a solution of ligand diethyl 2-hydroxyazulene-1,3-dicarboxylate (115.2 mg, 0.04 mmol) in MeOH (10 mL) was added KOH (0.04 mmol) in methanol (0.100 M) under stirring. The initially clear solution became cloudy due to the formation of the precipitate of the potassium salt of the deprotonated ligand. Methanol (10 mL) was added to the solution which was then heated until complete dissolution of the precipitates. $LnCl_3 \cdot nH_2O$ (0.01 mmol) (Ln = Pr, Nd, Gd, Ho, Er, Tm, Yb and Lu) in methanol (10 mL) was added to the resulting solution. This solution was stirred overnight and the resulting yellow precipitate was collected by filtration, washed three times with methanol and dried in vacuum over P_2O_5 for 48 h.

Data for KPr(Az)$_4$: 39.4 mg, 59% isolated yield; IR (KBr): $\tilde{\nu} = 2978$ (w), 1683 (s, $\nu_{C=O}$), 1615 (s, $\nu_{C=O}$), 1489 (s), 1454 (m), 1212 (m), 1147 (s), 803 cm^{-1} (m); ESI-MS (CH_2Cl_2 negative mode): m/z: 1289.2 $[M(Az)_4]^-$; elemental analysis calcd (%) for $C_{64}H_{60}O_{20}PrK \cdot CH_3OH$ (1361.22): C 57.35, H 4.74; found: C 57.42, H 4.49.

Data for KNd(Az)$_4$: 42.3 mg, 64% isolated yield; IR (KBr): $\tilde{\nu} = 2977$ (w), 1686 (s, $\nu_{C=O}$), 1615 (s, $\nu_{C=O}$), 1490 (s), 1454 (m), 1212 (m), 1148 (s), 803 cm^{-1} (m); ESI-MS (CH_2Cl_2 negative mode): m/z: 1289.2 $[M(Az)_4]^-$; elemental analysis calcd (%) for $C_{64}H_{60}O_{20}NdK \cdot CH_3OH$ (1364.55): C 57.21, H 4.73; found: C 57.45, H 4.54.

Data for KGd(Az)$_4$: 39.2 mg, 58% isolated yield; IR (KBr): $\tilde{\nu} = 2978$ (w), 1683 (s, $\nu_{C=O}$), 1616 (s, $\nu_{C=O}$), 1494 (s), 1455 (m), 1213 (m), 1151 (s), 803 cm^{-1} (m); ESI-MS (CH_2Cl_2 negative mode): m/z: 1306.2 $[M(Az)_4]^-$; elemental analysis calcd (%) for $C_{64}H_{60}O_{20}GdK \cdot CH_3OH$ (1377.56): C 56.67, H 4.68; found: C 56.45, H 4.39.

Data for KHo(Az)$_4$: 55.3 mg, 82% isolated yield; IR (KBr): $\tilde{\nu} = 2978$ (w), 1683 (s, $\nu_{C=O}$), 1616 (s, $\nu_{C=O}$), 1495 (s), 1471 (s), 1456 (m), 1213 (m), 1152 (s), 803 cm^{-1} (m); ESI-MS (CH_2Cl_2 negative mode): m/z: 1313.2 $[M(Az)_4]^-$; elemental analysis calcd (%) for $C_{64}H_{60}O_{20}HoK \cdot CH_3OH$ (1385.24): C 56.36, H 4.66; found: C 56.24, H 4.43.

Data for KEr(Az)$_4$: 47.4 mg, 70% isolated yield; IR (KBr): $\tilde{\nu} = 2978$ (w), 1683 (s, $\nu_{C=O}$), 1616 (s, $\nu_{C=O}$), 1495 (s), 1471 (s), 1455 (m), 1213 (m), 1151 (s), 803 cm^{-1} (m); ESI-MS (CH_2Cl_2 negative mode): m/z: 1316.2 $[M(Az)_4]^-$; elemental analysis calcd (%) for $C_{64}H_{60}O_{20}ErK \cdot CH_3OH$ (1387.57): C 56.26, H 4.65; found: C 56.26, H 4.41.

Data for KTm(Az)$_4$: 51.7 mg, 76% isolated yield; IR (KBr): $\tilde{\nu} = 2978$ (w), 1683 (s, $\nu_{C=O}$), 1616 (s, $\nu_{C=O}$), 1495 (s), 1481 (s), 1456 (m), 1213 (m), 1153 (s), 803 cm^{-1} (m); ESI-MS (CH_2Cl_2 negative mode): m/z: 1317.2 $[M(Az)_4]^-$; elemental analysis calcd (%) for $C_{64}H_{60}O_{20}TmK \cdot CH_3OH$ (1389.24): C 56.20, H 4.64; found: C 56.18, H 4.38.

Data for KYb(Az)$_4$: 45.0 mg, 66% isolated yield; ESI-MS (CH_2Cl_2 negative mode): m/z: 1322.2 $[M(Az)_4]^-$; IR (KBr): $\tilde{\nu} = 2976$ (w), 1685 (s, $\nu_{C=O}$), 1620 (s, $\nu_{C=O}$), 1495 (s), 1481 (m), 1455 (m), 1213 (m), 1152 (s), 803 cm^{-1} (m); elemental analysis calcd (%) for $C_{64}H_{60}O_{20}YbK \cdot CH_3OH$ (1393.35): C 56.03, H 4.63; found: C 56.14, H 4.30.

Data for KLu(Az)$_4$: 44.3 mg, 65% isolated yield; IR (KBr): $\tilde{\nu} = 2978$ (w), 1683 (s, $\nu_{C=O}$), 1622 (s, $\nu_{C=O}$), 1495 (s), 1480 (s), 1455 (m), 1213 (m), 1152 (s), 803 cm^{-1} (m); ESI-MS (CH_2Cl_2 negative mode): m/z: 1323.2 $[M(Az)_4]^-$; elemental analysis calcd (%) for $C_{64}H_{60}O_{20}LuK \cdot CH_3OH$ (1395.28): C 55.95, H 4.62; found: C 56.02, H 4.49.

Results and Discussion

Formation of ML$_4$ complexes: The lanthanide complexes were prepared by mixing for 15 h the deprotonated ligand with stoichiometric amounts of the lanthanide chloride in methanol at room temperature. The result of the elemental analysis suggests the formation of complexes with $KLn(Az)_4$ as molecular formula for all the lanthanide complexes studied (Ln = Pr, Nd, Gd, Ho, Er, Tm, Yb, Lu). This indicates that only one of the C=O groups of the ligand is coordinated to lanthanide cation forming a complex with ML_4 formula (the molecule acting as bidentate ligand, as shown in Scheme 2). This indication was confirmed by the FT-IR analysis. The IR absorption spectra of both the free ligand

and the complex have two different C=O stretching bands with one common and one different vibration frequency (Figure 1). The presence of two different C=O vibrations in

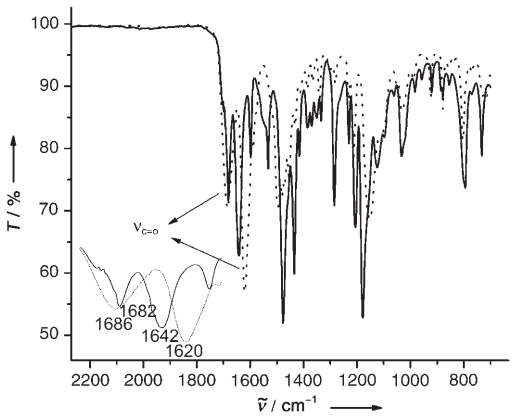

Figure 1. FT-IR spectra of the ligand HAz (——) and of the K[Yb(Az)] complex (•••••).

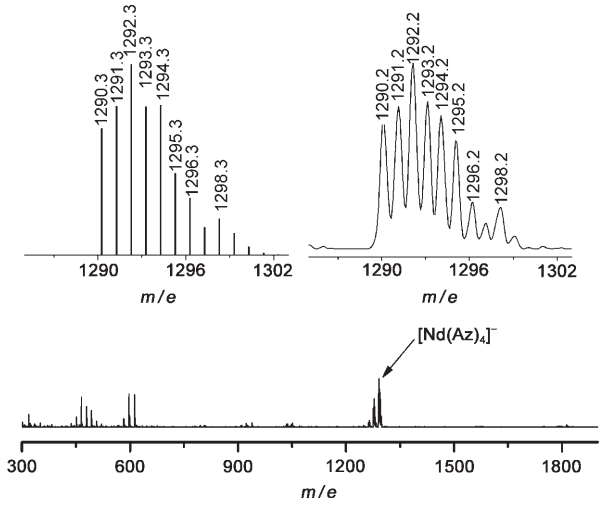

Figure 2. Bottom: ES-MS spectrum in negative mode at a concentration of ca. 10^{-4} M in CH_3CN/CH_2Cl_2 (top left, prediction of the isotopic distribution of the ML_4 peak; top right: the zoomed region of the experimental ML_4 peak).

the free ligand can be explained by the formation of a hydrogen bond between the OH group with one of the C=O group, which results in the red shift of the C=O stretching band. Similarly, the presence of different types of C=O vibrations in the coordinated ligand can be explained by one of the two C=O of the ligand being coordinated to the Ln^{3+} cation. The bands located at higher energy that appears at 1682 and 1686 cm^{-1} can be assigned to the ligand and to the Yb^{3+} complex respectively. This vibration frequency can be assigned to free C=O groups, which are not involved in the formation of hydrogen or coordination bonds. The vibration band located at lower wavenumber in the Yb complex (1620 cm^{-1}) is red-shifted by about 22 cm^{-1} compared to the value measured for the free ligand (1642 cm^{-1}), confirming the formation of a coordination bond between this C=O and the lanthanide cation.

Electrospray mass spectroscopy (ES-MS) measurements provide an insight on the nature of the species of complexes formed in solution. In the negative ion mode, the molecular peak corresponding to the $[Ln(Az)_4]^-$ anion is observed. The presence of signal assigned to the free ligand indicates partial dissociation of the complexes in these experimental conditions. The ES-MS spectrum of the Nd^{3+} complex is depicted as an example in Figure 2. It is important to point out that the relative abundance reflected by intensities in the MS spectra can not be directly used to interpret the relative amount of the species of complexes present in solution but allow to conclude the presence of the $[Ln(Az)_4]^-$ species.

Spectrophotometric titration: It has been shown by elemental analysis that the composition of the complexes corresponds to ML_4 when isolated in the solid state. To investigate the number and nature of the species formed between the ligand Az^- and the lanthanide cations in solution, UV/Vis spectrophotometric titrations were performed with Nd^{3+}, Er^{3+}, Tm^{3+} and Yb^{3+} cations. Spectra were collected varying the metal to ligand ratio in both CH_3CN and methanol solvents at constant ionic strength. UV/Vis spectra recorded during the spectrophotometric titration of a solution of the deprotonated ligand Az^- by Tm^{3+} in CH_3CN are depicted as example in the Figure 3. For all the four cations, a smooth evolution of the absorption spectra for Ln/Az^- in the range 0.1–1.0 with a single sharp endpoint for $Ln/Az^- = 4.0$ has been observed by monitoring the absorbance at 480 nm (Figure 3).

The software SPECFIT[48] was used to analyze the experimental data. Factor analysis indicated the presence of five independent colored species in solution. The data obtained from the titrations with the different cations were best fitted with a model where four complexes are successfully formed in solution: ML, ML_2, ML_3 and ML_4 and satisfactory stability constants were obtained using this model. Convergence of the fitting process to calculate $\log K_4$ values was only possible if the values of $\log K_1$, $\log K_2$ and $\log K_3$ were fixed to values of 9, 8 and 7, respectively, for the titrations performed in both MeOH and CH_3CN solvents. This could be explained by the high stability of the ML_1, ML_2 and ML_3 species formed in solution. A complementary explanation could be the strong correlation of the UV/Vis spectra of the individual species as indicated by the spectra of the individual ML_1, ML_2, ML_3 and ML_4 species calculated with the help of the Specfit software (see Figure S1, Supporting Information). $\log K_4$ stability constant values of 4.5 ± 0.3, 4.7 ± 0.3, 4.5 ± 0.3 and 4.1 ± 0.3 were obtained after fitting for Nd^{3+}, Er^{3+}, Tm^{3+} and Yb^{3+} complex, respectively, in CH_3OH, and 5.5 ± 0.3, 5.4 ± 0.3, 4.9 ± 0.3, 4.9 ± 0.3 were obtained from measurements in CH_3CN. The overall higher values of $\log K_4$ obtained in CH_3CN can be explained by this solvent being less coordinating than MeOH which posses an oxygen hard Lewis donor, resulting in lower competition be-

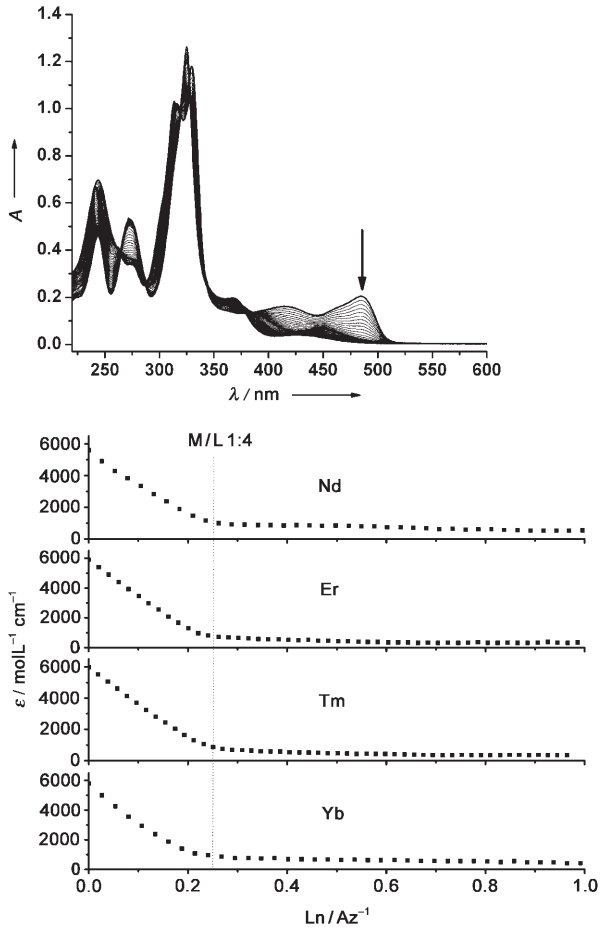

Figure 3. Top: Series of UV/Vis absorption spectra collected during the spectrophotometric titration of the deprotonated ligand Az^- in CH_3CN solution with Tm^{3+}. (Total ligand concentration: 3.42×10^{-5} mol L^{-1}; aliquots of $TmCl_3$ in CH_3CN were successively added (up to 1:1 metal to ligand ratio); $T=25.0\pm0.1$ °C; 0.01 M tetrabutylammonium perchlorate for ionic strength control). Bottom: Variations of observed molar extinctions at 484 nm in the titrations obtained with four lanthanide cations.

tween the ligand and this solvent. In addition, the titration spectra show a smooth evolution of the absorption spectra at 484 nm for Ln/Az^- in the range 0.1–1.0 with a single sharp end point for $Ln/Az^-=1:4$ (Figure 3). This series of results lead to the conclusion that four different lanthanide complexes ML_1, ML_2, ML_3 and ML_4 are successfully formed in MeOH solution. The values of $\log K_4$ for the ML_4 complexes are all comprised within the experimental error. A molecular modeling calculation (Figure 4) using MM3 parameters (CAChe)[51] also indicate that it is possible for four ligands to coordinate a central lanthanide cation. The qualitative analysis of the modeled structure indicates that these four ligands provide a good protection of the lanthanide cation from non-radiative deactivations from the environment.

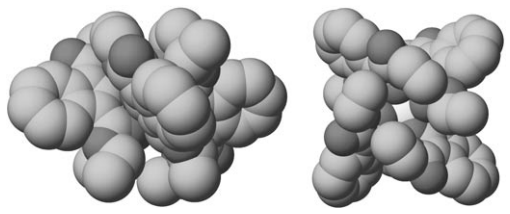

Figure 4. Two different views of the $[Yb(Az)_4]^-$ complex created with molecular modeling (MM3 parameters).

Photophysical properties of the ligand HAz: The UV/Vis absorption spectrum of the free ligand HAz in CH_3CN is reported in Figure 5. This spectrum indicates the presence of several electronic transitions with apparent maxima at 237, 261 and 311 nm with a shoulder located at 300 nm. There are two additional broader bands located at lower energy with an apparent maxima at 355 and 430 nm, which can be assigned to S_0–S_2 and S_0–S_1 transitions respectively (see below for the attribution of these bands).

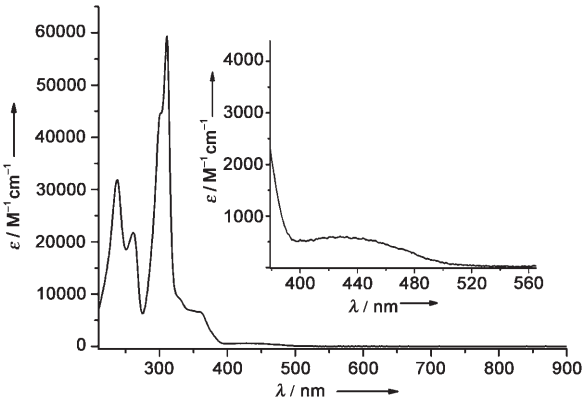

Figure 5. UV/Vis spectrum of the ligand HAz in CH_3CN (2.3×10^{-5} mol L^{-1} at room temperature). Inset: Zoomed region of the absorption band centered at 430 nm.

In contrast to the blue color of azulene, the ligand HAz is yellowish orange. It is known that the electronic structure and photophysical properties of derivatives of azulene are affected by their substituents.[52] This perturbation of the molecular orbitals of the azulene moiety can be rationalized by a qualitative pictorial description of the low lying molecular orbitals (Figure 6).[53] The HOMO, LUMO, and LUMO+1 orbitals of azulene, which correspond to S_0, S_1 and S_2 levels, respectively, are depicted in the Figure 6.

For azulene, the small overlap between HOMO and LUMO leads to a transition located at lower energy of the S_1 state. The large electron–electron correlation energy for the LUMO+1 and HOMO considerably raises the energy of the second singlet excited state (S_2 level of azulene). As a result, the S_2 (raised in electronic energy level) and S_1 (lowered in electronic energy levels) couple together to create a unusually large gap resulting the so called "blue window" (360–450 nm) of azulene,[53] which provides to this compound its blue color.

There are three substituents on the ligand HAz, two C=O groups and one OH group. The C=O group is a conjugative, electron-withdrawing substituent and it generates two opposing effects on the electron densities at C-1 and C-3 of

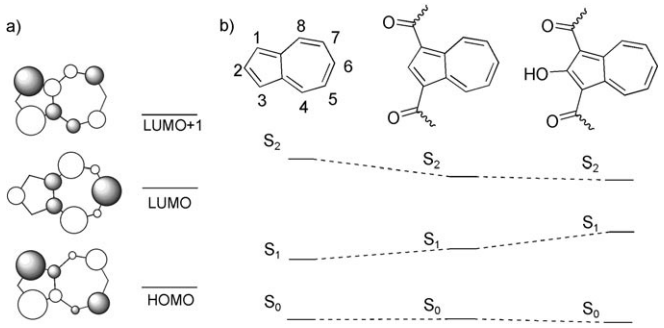

Figure 6. a) Probability of location of the electron in the HOMO, LUMO and LUMO+1 of azulene;[53] b) schematic illustration of effects of different substituents on the energies of electronic levels of azulene.

the azulene moiety HOMO to stabilize or destabilize the molecular orbitals. It has been found that the aldehyde group causes a blue shift of the S_1 state because of its inductive electron withdrawing effect, but causes red shift of the S_2 state due to the conjugation effect.[52] On the other hand, the hydroxyl group at C-2, which is a resonance donating group, will destabilize the LUMO orbital of azulene. This will lead to an increased S_0–S_1 gap and to a corresponding blue shift, which explains why the energy position of the maximum of the S_0–S_1 transition of 1,3-dicarboxaldehyde azulene is at approximately 500 nm (20000 cm^{-1}), while it is around 428 nm for our ligand. The red-shift of the band corresponding to S_2 results in the diminished transmission of blue light (near 400 nm), and a simultaneous increase in transmittance of red/yellow light, therefore, the ligand is orange.

Coordinated ligand-centered luminescence in $KGd(Az)_4$: The UV/Vis absorption spectra of the different lanthanide complexes studied in this work were measured in CH_3CN at room temperature (Figure S2 in Supporting Information). They are similar to each other since the energy location of these bands all reflect the electronic structure of the ligands bound to a central lanthanide cation. The spectrum of the Gd^{3+} complex is shown in Figure 7 as an example. Compared with the free ligand, the $\pi\rightarrow\pi^*$ transition band in the UV/Vis spectrum red-shifts from 428 nm (in the free ligand) to 452 nm in the complex with an increased molar absorptivity. This can be attributed to the perturbation of the electronic structure of the ligand upon metal ion coordination, making this transition more allowed compared to the free ligand.

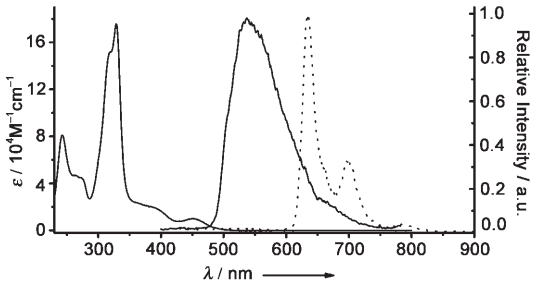

Figure 7. UV/Vis absorption (——), normalized fluorescence (——) and phosphorescence (·····) spectra of $KGd(Az)_4$ in CH_3CN (UV/Vis: room temperature; fluorescence: $M=1.2\times10^{-5}$ mol^{-1} L^{-1}, $\lambda_{ex}=400$ nm, 298 K; phosphorescence: $\lambda_{ex}=400$ nm, 77 K, delay time 0.01 ms, gate time 20 ms).

The fluorescence of the free ligand HAz is faint. No phosphorescence of the free ligand was detectable at 77 K. However, it has been possible to record the steady-state fluorescence and time-resolved phosphorescence bands arising from the ligand bound to Gd^{3+} in the $KGd(Az)_4$ complex (Figure 7). There is no ligand to lanthanide energy transfer in this complex because the Gd^{3+} electronic levels are too high in energy to accept energy from the singlet and/or triplet states of the ligand. The location of these bands in both types of spectra is helpful to identify the energy of the singlet and triplet states of the ligands bound to lanthanide metal ions. The fluorescence spectrum obtained upon excitation of the ligand at room temperature resulted in the presence of a broad ligand-centered band that is assigned to the S_1–S_0 transition with an apparent maximum of the electronic envelope at 18700 cm^{-1} (536 nm). In time-resolved mode, when a delay (0.01 ms) is applied after the excitation flash to record the phosphorescence spectrum, the fluorescence band disappears and is replaced by a phosphorescence signal containing three bands with apparent maxima located at 15700 cm^{-1} (635 nm), 14306 cm^{-1} (699 nm) and 12700 cm^{-1} (788 nm). A similar pattern is also observed for the $KGd(Trop)_4$ complex (Table 1 and Figure S3, Supporting Information), which can be attributed to the partial similarity between the electronic structures of these two molecules. This set of bands is attributed to the phosphorescence arising from the triplet state of the bound ligand. In comparison to the energy of the triplet state reported for azulene 13600 cm^{-1} (733 nm), the triplet state of the ligand is significantly blue-shifted if we consider the maxima of the bands located at 15700 and 14300 cm^{-1}. This is due to the presence of the two substituents, which are required for the coordination of the lanthanide cations. Nevertheless, the triplet state of this ligand is still located at relatively low energy compared with the tropolonate ligand and most other ligands used for sensitization of NIR emitting lanthanide cations.

Table 1. Comparison of singlet and triplet state energies (cm^{-1}) for the Tropolonate and Az^- ligands.

	$KGd(Az)_4$			$KGd(Trop)_4$		
singlet[a]		18700			23500	
triplet[b]	15700	14300	12700	17200	15600	14300

[a] Steady state fluorescence spectra recorded at 298 K (10^{-5} mol L^{-1} in CH_3CN and DMSO for $KGd(Az)_4$ and $KGd(Trop)_4$, respectively). [b] Time-resolved phosphorescence spectra recorded on solid samples at 77 K.

Sensitization of lanthanide-centered near-infrared emission: Remarkably, the Az ligands can sensitize four different NIR

emitting Ln^{3+} (Ln = Yb, Nd, Er, and Tm) in $Ln(Az)_4$ complexes in CH_3CN at room temperature. The luminescence spectra of these four different lanthanide complexes are depicted in Figure 8. Through excitation of the absorption

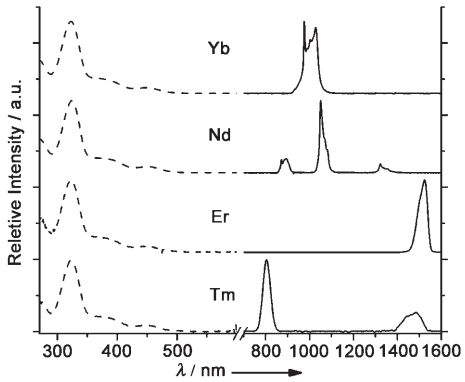

Figure 8. Normalized excitation (dashed line) and emission spectra (plain line) of four different lanthanide complexes 10^{-5} mol^{-1} L^{-1} in CH_3CN (λ_{ex} = 380 nm).

bands of the coordinated ligand, the solution of Yb^{3+} complex displays a NIR emission band ranging from 976 to 1028 nm, which is assigned to the $^2F_{5/2} \rightarrow {}^2F_{7/2}$ transition. For the Nd^{3+} complex, emission bands were observed at 895, 1051, and 1323 nm and are attributed to the transitions from the $^4F_{3/2}$ level to the $^4I_{9/2}$, $^4I_{11/2}$ and $^4I_{13/2}$ sublevels respectively. For Er^{3+} complex, the emission band observed at 1524 nm can be assigned to the transition from the $^4I_{13/2}$ level to $^4I_{15/2}$ level. Tm^{3+} emission is not frequently observed for lanthanide complexes in solution. In CH_3CN solution, two transitions were observed at 803 and 1487 nm. They are assigned to $^3F_4 \rightarrow {}^3H_6$ and $^3F_4 \rightarrow {}^3H_4$ transitions respectively. The emission wavelengths of the Nd^{3+}, Yb^{3+} and Tm^{3+} complexes are in a spectral range well suited for bioanalytical assays (minimization of the absorption by the biological system).[25] As shown in Figure 8, there is only slight overlap between these emission spectra, allowing the potential for multiplex measurements. Attempts to generate Ho^{3+} and Pr^{3+} luminescence upon ligand L excitation were unsuccessful.

To quantify the intramolecular ligand to metal ion energy transfer efficiency in the different lanthanide complexes, luminescence quantum yields were measured in CH_3CN and CD_3CN upon ligand excitation using $KYb(Trop)_4$ as reference.[34] Three different excitation wavelengths corresponding to three maxima of the absorption spectra at 320, 380 and 447 nm, respectively, were used systematically. The results are reported in Table 2. The quantum yield values recorded with different excitation wavelengths are all within the experimental error (5–17 %). Therefore, it is suggested that a unique path of energy is used for the sensitization of all the lanthanide cations studied by the chromophoric ligand. This assumption is supported by the fact that all the excitation spectra are similar to each other (Figure 8) and are well matched to the corresponding absorption spectra

Table 2. Absolute quantum yield values of lanthanide complexes at 298 K in CH_3CN and CD_3CN at different excitation wavelength.

Ln	Wavelength [nm]	CH_3CN[a]	CD_3CN[a]
Yb	322[a]	$2.7(2)\times10^{-2}$	$3.1(2)\times10^{-2}$
	375[b]	$3.8(2)\times10^{-2}$	$4.2(2)\times10^{-2}$
	447[c]	$3.2(2)\times10^{-2}$	$3.6(2)\times10^{-2}$
Nd	322[a]	$4.0(2)\times10^{-3}$	$4.7(4)\times10^{-3}$
	383[b]	$4.5(3)\times10^{-3}$	$5.3(3)\times10^{-3}$
	449[c]	$3.7(2)\times10^{-3}$	$4.9(2)\times10^{-3}$
Er	322[a]	$2.0(1)\times10^{-4}$	$2.2(1)\times10^{-4}$
	387[b]	$2.1(1)\times10^{-4}$	$2.4(1)\times10^{-4}$
	447[c]	$1.8(1)\times10^{-4}$	$2.2(1)\times10^{-4}$
Tm	320[a]	$4.3(2)\times10^{-5}$	$5.1(1)\times10^{-5}$
	380[b]	$5.9(2)\times10^{-5}$	$6.6(1)\times10^{-5}$
	446[c]	$4.9(2)\times10^{-5}$	$6.5(2)\times10^{-5}$

[a] 1.7×10^{-5} mol L^{-1}. [b] 1×10^{-4} mol L^{-1}. [c] 2×10^{-4} mol L^{-1}.

(Figure S2, Supporting Information). Notably this observation was possible for all four NIR emitting lanthanide cations sensitized by Az^- despite the fact that the luminescent Yb^{3+}, Nd^{3+}, Er^{3+}, and Tm^{3+} cations have different energies of accepting levels. It can be concluded that the excitation has the same efficiency for all three absorbance bands for all four lanthanide cations as the quantum yield values do not depend on the excitation wavelengths.

The quantum yield of the Yb^{3+} complex is especially large with values of 3.8 % in CH_3CN and 4.2 % in CD_3CN, compared with the value reported for other Yb^{3+} complexes in solution, such as 3.2 and 2.4 % reported for a monoporphyrinate complex in CH_2Cl_2,[11] 1.9 % for our tropolonate complex in DMSO,[34] 0.5 % for a terphenyl-based complex in DMSO,[54] 1.8 % for a bimetallic helicate in D_2O,[55] or 0.45 % for fluorexon complex in D_2O.[56] Although smaller, the quantum yield of the Nd^{3+} complex (0.45 % in CH_3CN and 0.53 % in CD_3CN) is also high compared with other Nd^{3+} complexes with 0.2 % for monoporphyrinate complexes in CH_2Cl_2,[11] 0.21 % for tropolonate Nd^{3+} complex in DMSO,[34] 0.038 % for the Nd-fluorexon complex in D_2O,[56] 0.075 % for 8-hydroxyquinolinate-based Nd^{3+} complex in D_2O.[23]

The luminescent lifetimes have been recorded in order to evaluate the coordination environment around the lanthanide cations in these complexes in solution and to quantify the degree of protection against non-radiative deactivation provided by the four Az^- ligands around the central lanthanide cation. The luminescence decays of the Yb^{3+} and Nd^{3+} complexes in different solvents were measured and fit as monoexponential decays in all the studied solvents (Table 3). This indicates that a unique and consistent coordination environment is present around the lanthanide in the complex.

Table 3. Luminescence lifetimes (μs) of $[Nd(Az)_4]^-$ and $[Yb(Az)_4]^-$ complexes in different solvents (298 K, 2×10^{-5} mol L^{-1}).

	MeOH	CD_3OD	CH_3CN	CD_3CN
Yb^{3+}	12.01 ± 0.07	33.71 ± 0.03	24.61 ± 0.01	32.81 ± 0.12
Nd^{3+}	0.37 ± 0.01	1.33 ± 0.01	1.85 ± 0.01	2.68 ± 0.01

The comparison between the luminescence lifetimes in deuterated and non-deuterated solvents can be used to quantify the number of solvent molecules coordinated to the lanthanide cations in solution. The calculation of the hydration/solvation number is obtained by using an empirical Equation (1). This formula was first developed by Horrocks et al.[57,58] In this formula, q is the number of water molecules bound to lanthanide ion in the first sphere of coordination; k_H and k_D are the rate constants of excited states of lanthanide ion in H_2O and D_2O, respectively. A is a proportionality constant related to the sensitivity of the lanthanide ion to vibrational quenching by OH oscillators, B is the correction factor for outer sphere water molecules.

$$q = A(k_H - k_D) - B \quad (1)$$

More recently, Beeby et al. modified this formula for the determination of q for Yb^{3+} and Nd^{3+} complexes in MeOH solution,[59,60] in which $A = 0.29$ μs (Nd^{3+}) or 2 μs (Yb^{3+}), $B = 0.4$ (Nd^{3+}) or 0.1 (Yb^{3+}), $k_H = 1/\tau_H$ and $k_D = 1/\tau_D$ are given in μs^{-1}.

Applying these formulas, q values of −0.05 and 0.16 were calculated for the Yb^{3+} and Nd^{3+} complexes, respectively. These near-zero values indicate that there are no water/solvent molecules bound to the lanthanide ion in the first coordination sphere for $[Ln(Az)_4]^-$ in solution. This is consistent for both the larger Nd^{3+} (Shannon's effective ionic radius: 1.109 Å[61]) and smaller Yb^{3+} (Shannon's effective ionic radius: 0.985 Å[61]) cations. Therefore, we can conclude that the four bidentate ligands efficiently protect Ln^{3+} cations against nonradiative deactivations induced by solvent molecules. The azulene complexes provide superior protection compared with the ML_4 tropolonate complexes,[34] where one solvent molecule is bound to the central lanthanide cation. It also confirms the results of elemental analysis that four Az^- ligands are bound to the central lanthanide cation in $[Ln(Az)_4]^-$ providing a lanthanide coordination number of 8. The luminescence lifetime obtained for the Yb^{3+} complex in acetonitrile solution (24.61 μs) is fairly long compared to the value obtained in MeOH (12.01 μs) and the typical average value around 10 μs reported for most Yb^{3+} complexes described in the literature.[23,62,63] This luminescence lifetime is similar to Yb^{3+} in CD_3OD and CD_3CN, an indication that the non-radiative quenching is similar for the Yb^{3+} complex in both solvents. On the other hand, the luminescence lifetimes of the Nd^{3+} complex in these two solvents are very different, 1.33 and 2.68 μs in CD_3OD and CD_3CN, respectively. This indicates that Nd^{3+} is more sensitive to high energy oscillations than Yb^{3+}. The main difference between these two solvents is the O-D group in CD_3OD, which has vibrational energy around 2500 cm^{-1}, versus the CN group in CD_3CN, which has a vibrational energy of 2250 cm^{-1}. Nd^{3+} has more electronic states at high energy than Yb^{3+}, which increases the probability of quenching.

Conclusion

In summary, lanthanide complexes $[Ln(Az)_4]^-$ formed by reaction of one lanthanide cation with four azulene-based ligands, HAz, have been isolated and characterized in solid state and in solution. Their photophysical properties have been analyzed, with a specific interest for the sensitization of near-infrared lanthanide cations. It was hypothesized that, due to its triplet state located at lower energy compared to the tropolonate ligand previously studied in our group, the HAz ligand would be more efficient in sensitizing several lanthanide cations.

Spectrophotometric titrations indicated that four Az^- react successively with one lanthanide cation to form a ML_4 type of complex in solution. The investigation of the photophysical properties of $[Ln(Az)_4]^-$ shows that Az^- sensitize efficiently four different NIR emitting lanthanide cations, Nd^{3+}, Er^{3+}, Yb^{3+}, and Tm^{3+}. The analysis of luminescence lifetimes of the lanthanide cations recorded in deuterated and non-deuterated solvents indicated that no solvent molecules are bound to the lanthanide cation in the $[Ln(Az)_4]^-$ complexes formed with $Ln = Nd^{3+}$ and Yb^{3+}. This efficient protection of the lanthanide cation against non-radiative deactivations results from the coordination the four ligands Az^- to the central lanthanide cation. As a result, the luminescence lifetimes of the Nd^{3+} and Yb^{3+} complexes are significantly longer in comparison to the values reported in the literature for most near-infrared emitting lanthanide complexes in solution. The quantum yields of the Nd^{3+} and Yb^{3+} complexes are among the highest values reported for NIR emitting lanthanide complexes in solution, which we attribute to a combination of efficient ligand to lanthanide energy transfer and good protection of the lanthanide cations. The fact that the azulene based ligand can sensitize not only Yb^{3+}, Nd^{3+}, and Er^{3+}, but also Tm^{3+} indicates that it is a promising sensitizer for NIR lanthanide ion, potentially suitable for biological imaging. A sensitizer that provides the advantage of a unique excitation wavelength (unique instrumental source) to obtain four different emission wavelengths is an important advantage for multiplex assays. To provide applicability to this system, the ligand design will be modified to obtain solubility in water and to increase the stability of the complex in solution by increasing denticity of this ligand.

Acknowledgements

Funding was provided through the University of Pittsburgh and through the National Science Foundation (award DBI0352346). J.Z. was supported through an Andrew Mellon Predoctoral Fellowship.

[1] J.-C. G. Bünzli, *Acc. Chem. Res.* **2006**, *39*, 53–61.
[2] J.-C. G. Bünzli, C. Piguet, *Chem. Soc. Rev.* **2005**, *34*, 1048–1077.
[3] A. Beeby, R. S. Dickins, S. Faulkner, D. Parker, J. A. G. Williams, *Chem. Commun.* **1997**, 1401–1402.
[4] C. L. Maupin, D. Parker, J. A. G. Williams, J. P. Riehl, *J. Am. Chem. Soc.* **1998**, *120*, 10563–10564.

[5] M. P. O. Wolbers, F. C. J. M. van Veggel, B. H. M. Snellink-Ruel, J. W. Hofstraat, F. A. J. Guerts, D. N. Reinhoudt, *J. Chem. Soc. Perkin Trans. 2* **1998**, 2141–2150.
[6] A. Beeby, R. S. Dickins, S. FitzGerald, L. J. Govenlock, D. Parker, J. A. G. Williams, C. L. Maupin, J. P. Riehl, G. Siligardi, *Chem. Commun.* **2000**, 1183–1184.
[7] Y. Hasegawa, T. Ohkubo, K. Sogabe, Y. Kawamura, Y. Wada, N. Nakashima, S. Yanagida, *Angew. Chem.* **2000**, *112*, 365–368; *Angew. Chem. Int. Ed.* **2000**, *39*, 357–360.
[8] M. H. V. Werts, R. H. Woudenberg, P. G. Emmerink, R. van Gassel, J. W. Hofstraat, J. W. Verhoeven, *Angew. Chem.* **2000**, *112*, 4716–4718; *Angew. Chem. Int. Ed.* **2000**, *39*, 4542–4544.
[9] D. Imbert, M. Cantuel, J.-C. G. Bünzli, G. Bernardinelli, C. Piguet, *J. Am. Chem. Soc.* **2003**, *125*, 15698–15699.
[10] G. A. Hebbink, L. Grave, L. A. Woldering, D. N. Reinhoudt, F. C. J. M. van Veggel, *J. Phys. Chem. A* **2003**, *107*, 2483–2491.
[11] T. J. Foley, B. S. Harrison, A. S. Knefely, K. A. Abboud, J. R. Reynolds, K. S. Schanze, J. M. Boncella, *Inorg. Chem.* **2003**, *42*, 5023–5032.
[12] S. J. A. Pope, B. J. Coe, S. Faulkner, E. V. Bichenkova, X. Yu, K. T. Douglas, *J. Am. Chem. Soc.* **2004**, *126*, 9490–9491.
[13] R. Van Deun, P. Fias, P. Nockemann, A. Schepers, T. N. Parac-Vogt, K. Van Hecke, L. Van Meervelt, K. Binnemans, *Inorg. Chem.* **2004**, *43*, 8461–8469.
[14] A. P. Bassett, R. Van Deun, P. Nockemann, P. B. Glover, B. M. Kariuki, K. Van Hecke, L. Van Meervelt, Z. Pikramenou, *Inorg. Chem.* **2005**, *44*, 6140–6142.
[15] S. Banerjee, L. Huebner, M. D. Romanelli, G. A. Kumar, R. E. Riman, T. J. Emge, J. G. Brennan, *J. Am. Chem. Soc.* **2005**, *127*, 15900–15906.
[16] S. Comby, D. Imbert, A.-S. Chauvin, J.-C. G. Bünzli, *Inorg. Chem.* **2006**, *45*, 732–743.
[17] W.-K. Lo, W.-K. Wong, W.-Y. Wong, J. Guo, K.-T. Yeung, Y.-K. Cheng, X. Yang, R. A. Jones, *Inorg. Chem.* **2006**, *45*, 9315–9325.
[18] L. Bertolo, S. Tamburini, P. A. Vigato, W. Porzio, G. Macchi, F. Meinardi, *Eur. J. Inorg. Chem.* **2006**, 2370–2376.
[19] L. N. Sun, J. B. Yu, G. L. Zheng, H. J. Zhang, Q. G. Meng, C. Y. Peng, L. S. Fu, F. Y. Liu, Y. N. Yu, *Eur. J. Inorg. Chem.* **2006**, 3962–3973.
[20] R. Van Deun, P. Fias, P. Nockemann, K. Van Hecke, L. Van Meervelt, K. Binnemans, *Inorg. Chem.* **2006**, *45*, 10416–10418.
[21] T. Lazarides, M. A. H. Alamiry, H. Adams, S. J. A. Pope, S. Faulkner, J. A. Weinstein, M. D. Ward, *Dalton Trans.* **2007**, 1484–1491.
[22] T. K. Ronson, T. Lazarides, H. Adams, S. J. A. Pope, D. Sykes, S. Faulkner, S. J. Coles, M. B. Hursthouse, W. Clegg, R. W. Harrington, M. D. Ward, *Chem. Eur. J.* **2006**, *12*, 9299–9313.
[23] S. Comby, D. Imbert, C. Vandevyver, J.-C. G. Bünzli, *Chem. Eur. J.* **2007**, *13*, 936–944.
[24] S. Kim, Y. T. Lim, E. G. Soltesz, A. M. De Grand, J. Lee, A. Nakayama, J. A. Parker, T. Mihaljevic, R. G. Laurence, D. M. Dor, L. H. Cohn, M. G. Bawendi, J. V. Frangioni, *Nat. Biotechnol.* **2004**, *22*, 93–97.
[25] R. Weissleder, V. Ntziachristos, *Nat. Med.* **2003**, *9*, 123–128.
[26] S. Stolik, J. A. Delgado, A. Perez, L. Anasagasti, *J. Photochem. Photobiol. B* **2000**, *57*, 90–93.
[27] T. Jüstel, D. U. Wiechert, C. Lau, D. Sendor, U. Kynast, *Adv. Funct. Mater.* **2001**, *11*, 105–110.
[28] T.-S. Kang, B. S. Harrison, T. J. Foley, A. S. Knefely, J. M. Boncella, J. R. Reynolds, K. S. Schanze, *Adv. Mater.* **2003**, *15*, 1093–1097.
[29] L. H. Slooff, A. Polman, M. P. Oude Wolbers, F. C. J. M. van Veggel, D. N. Reinhoudt, J. W. Hofstraat, *J. Appl. Phys.* **1998**, *83*, 497–503.
[30] L. H. Slooff, A. van Blaaderen, A. Polman, G. A. Hebbink, S. I. Klink, F. C. J. M. Van Veggel, D. N. Reinhoudt, J. W. Hofstraat, *J. Appl. Phys.* **2002**, *91*, 3955–3980.
[31] S. I. Weissman, *J. Chem. Phys.* **1942**, *10*, 214–217.
[32] C. Yang, L.-M. Fu, Y. Wang, J.-P. Zhang, W.-T. Wong, X.-C. Ai, Y.-F. Qiao, B.-S. Zou, L.-L. Gui, *Angew. Chem.* **2004**, *116*, 5120–5123; *Angew. Chem. Int. Ed.* **2004**, *43*, 5010–5013.
[33] G. A. Hebbink, S. I. Klink, L. Grave, P. G. B. Oude Alink, F. C. J. M. Van Veggel, *ChemPhysChem* **2002**, *3*, 1014–1018.
[34] J. Zhang, P. D. Badger, S. J. Geib, S. Petoud, *Angew. Chem.* **2005**, *117*, 2564–2568; *Angew. Chem. Int. Ed.* **2005**, *44*, 2508–2512.
[35] J. E. Frey, A. M. Andrews, S. D. Combs, S. P. Edens, J. J. Puckett, R. E. Seagle, L. A. Torreano, *J. Org. Chem.* **1992**, *57*, 6460–6466.
[36] S. Schmitt, M. Baumgarten, J. Simon, K. Hafner, *Angew. Chem.* **1998**, *110*, 1129–1133; *Angew. Chem. Int. Ed.* **1998**, *37*, 1077–1081.
[37] F. Wang, Y.-H. Lai, M.-Y. Han, *Macromolecules* **2004**, *37*, 3222–3230.
[38] M. Porsch, G. Sigl-Seifert, J. Daub, *Adv. Mater.* **1997**, *9*, 635–639.
[39] S. Ito, H. Inabe, N. Morita, K. Ohta, T. Kitamura, K. Imafuku, *J. Am. Chem. Soc.* **2003**, *125*, 1669–1680.
[40] S. E. Estdale, R. Brettle, D. A. Dummur, C. M. Marson, *J. Mater. Chem.* **1997**, *7*, 391–401.
[41] T. Zielinski, M. Kedziorek, J. Jurczak, *Tetrahedron Lett.* **2005**, *46*, 6231–6234.
[42] H. Salman, Y. Abraham, S. Tal, S. Meltzman, M. Kapon, N. Tessler, S. Speiser, Y. Eichen, *Eur. J. Org. Chem.* **2005**, 2207–2212.
[43] T. Mrozek, H. Gorner, J. Daub, *Chem. Eur. J.* **2001**, *7*, 1028–1040.
[44] P. G. Lacroix, I. Malfant, G. Iftime, A. C. Razus, K. Nakatani, J. A. Delaire, *Chem. Eur. J.* **2000**, *6*, 2599–2608.
[45] L. Cristian, I. Sasaki, P. G. Lacroix, B. Donnadieu, I. Asselberghs, K. Clays, A. C. Razus, *Chem. Mater.* **2004**, *16*, 3543–3551.
[46] C. Lambert, G. Noell, M. Zabel, F. Hampel, E. Schmaelzlin, C. Braeuchle, K. Meerholz, *Chem. Eur. J.* **2003**, *9*, 4232–4239.
[47] W. G. Herkstroeter, *J. Am. Chem. Soc.* **1975**, *97*, 4161–4167.
[48] H. Gampp, M. Maeder, C. J. Meyer, A. D. Zuberbuehler, *Talanta* **1985**, *32*, 1133–1139.
[49] R. Brettle, D. A. Dunmur, S. Estdale, C. M. Marson, *J. Mater. Chem.* **1993**, *3*, 327–331.
[50] W. v. E. Doering, L. H. Knox, *J. Am. Chem. Soc.* **1952**, *74*, 5683–5687.
[51] F. L. CAChe WorkSystem Pro Version 6.1.12.33, Fujitsu America Inc,. USA, **2000–2004**.
[52] G. Eber, F. Grueneis, S. Schneider, F. Doerr, *Chem. Phys. Lett.* **1974**, *29*, 397–404.
[53] R. S. H. Liu, A. E. Asato, *J. Photochem. Photobiol. C* **2003**, *4*, 179–194.
[54] S. I. Klink, G. A. Hebbink, L. Grave, F. C. J. M. van Veggel, D. N. Reinhoudt, L. H. Slooff, A. Polman, J. W. Hofstraat, *J. Appl. Phys.* **1999**, *86*, 1181–1185.
[55] F. R. Goncalves e Silva, O. L. Malta, C. Reinhard, H.-U. Güdel, C. Piguet, J. E. Moser, J.-C. G. Bünzli, *J. Phys. Chem. A* **2002**, *106*, 1670–1677.
[56] M. H. V. Werts, J. W. Verhoeven, J. W. Hofstraat, *Perkin 2* **2000**, 433–439.
[57] W. D. Horrocks, Jr., D. R. Sudnick, *J. Am. Chem. Soc.* **1979**, *101*, 334–340.
[58] W. D. Horrocks, Jr., D. R. Sudnick, *Acc. Chem. Res.* **1981**, *14*, 384–392.
[59] G. M. Davies, R. J. Aarons, G. R. Motson, J. C. Jeffery, H. Adams, S. Faulkner, M. D. Ward, *Dalton Trans.* **2004**, 1136–1144.
[60] A. Beeby, B. P. Burton-Pye, S. Faulkner, G. R. Motson, J. C. Jeffery, J. A. McCleverty, M. D. Ward, *J. Chem. Soc. Dalton Trans.* **2002**, 1923–1928.
[61] R. D. Shannon, *Acta Crystallogr. Sect. A* **1976**, *32*, 751–767.
[62] S. I. Klink, H. Keizer, F. C. J. M. van Veggel, *Angew. Chem.* **2000**, *112*, 4489–4491; *Angew. Chem. Int. Ed.* **2000**, *39*, 4319–4321.
[63] N. M. Shavaleev, L. P. Moorcraft, S. J. A. Pope, Z. R. Bell, S. Faulkner, M. D. Ward, *Chem. Eur. J.* **2003**, *9*, 5283–5291.

Received: July 12, 2007
Published online: November 28, 2007

